J. Plasma Fusion Res. SERIES, Vol. 4 (2001) 75–81

Control of Radial Electric Field and Low-Frequency Fluctuations in Open-Ended Systems

INUTAKE Masaaki*
Tohoku University, Sendai 980-8579, Japan

(Received: 5 December 2000 / Accepted: 27 October 2001)

Abstract

Both drift mode and flute mode instabilities are found to depend sensitively on radial electric field strength in the GAMMA10 tandem mirror, when the electric field is controlled by use of end-plate biasing. In order to clarify effects of both radial electric field and its shear on low-frequency fluctuations, systematic experiments and precise measurements have been done in a small linear device, Q_T-U of Tohoku University. Drift-mode fluctuations depend on both radial electric field and its shear. The drift-mode is destabilized in the region of weakly negative electric field. In the strong E_r region, the mode is suppressed, irrespective of its sign. This behavior agrees qualitatively with that observed in the ECH mode of GAMMA10. The drift-mode in the Q_T-U is clearly stabilized by the increase in the net ion drift shear which is defined as the sum of $\boldsymbol{E} \times \boldsymbol{B}$ drift shear and ion diamagnetic drift shear. Flute-mode observed in the Q_T-U is identified as Kelvin-Helmholtz instability driven by strong $\boldsymbol{E} \times \boldsymbol{B}$ drift shear.

Keywords:

open system, tandem mirror, end plate biasing, electric field shear, flow shear stabilization, drift wave, Kelvin-Helmholtz instability

1. Introduction

Effect of radial electric field and its shear on low-frequency fluctuations has been investigated since the so-called H/L mode-transition of improving radial confinement was found in both open and closed systems [1-3]. Biased-electrode experiments have been performed in linear devices [4-7] and also in toroidal devices [8,9] in order to control radial potential profiles and fluctuations. Radial potential control in the GAMMA10 tandem mirror [10] is very effective to suppress low-frequency fluctuations [11,12] and to achieve a stable plasma with hot ion temperature of up to 10 keV [13]. It is found in GAMMA10 that both flute mode and drift mode instabilities depend sensitively on radial electric field strength.

It is not yet clarified which is the most effective for suppressing fluctuations and improving radial confinement in a fusion-oriented device, electric field or electric field shear. This may be caused by the difficulty of measuring precisely radial electric field profile and identifying instabilities concerned with radial transport in large-scale fusion-oriented devices. Furthermore, when qualitatively comparing with experiment, it often is necessary to account for the radial character of the electric field in cylindrical geometry. However, a kinetic theory on the transverse electric field shear effects on a drift mode is available only for slab geometry. In a slab geometry, the transverse electric field shear increases with the increase of the electric field shear with a fixed shear length. In experiments, this situation is not necessarily true. Therefore, basic experiments have been done under various combinations of the electric field and its shear in order to discriminate both effects of the

*Corresponding author's e-mail: inutake@ecei.tohoku.ac.jp

rotation and the rotation shear.

In order to investigate effects of both radial electric field and its shear on low-frequency fluctuations, basic experiments have been carried out in a small linear device, Q_T-U of Tohoku University, in which systematic control and precise measurements of radial potential profile can be done [14,15].

Numerous theoretical works have been done for transverse electric-field shear driven Kelvin-Helmholtz (KH) modes [16-19] in both slab and cylindrical geometry, to explain the laboratory experiments in the Q-machine [5,20] and the observation in space plasmas. The effects of transverse electric-field shear on drift modes are also theoretically studied [21-23] in slab geometry. In a tandem mirror with a parabolic potential profile, a rotation-driven drift and flute mode is predicted to be destabilized but has a stable window around the rotation frequency shifted by the electron and ion diamagnetic frequency, respectively [24]. To explain shear-driven instabilities in space plasmas and related laboratory experiments [25,26], inhomogeneous energy-density-driven (IEDD) instability mechanism [27] are proposed and compared with KH instabilities in slab and cylindrical geometry [28]. The IEDD mechanism is also studied for ion-cyclotron, ion-acoustic and drift modes in slab geometry [29].

In this paper, results of radial electric field E_r control in the GAMMA10 and the Q_T-U devices are presented and compared with each other.

2. Radial Electric Field Control in the GAMMA10 Tandem Mirror

2.1 GAMMA10 Tandem Mirror

GAMMA10 consists of an axi-symmetric central cell for confining a main plasma, anchor cells with minimum-B field for suppressing MHD instabilities, and axisymmetric end mirrors for forming both plug/thermal barrier [30], as shown schematically in Fig.1. At each end is provided a segmented end-plate, which consists of five concentric annular rings, electrically insulated with each other. The innermost ring is called #1 and the outermost #5. Each segment of the end plates is conventionally floated electrically from the vacuum vessel through 1 MΩ resistor and can be biased arbitrarily at a voltage to control radial electric field E_r in the confining region. The radial electric field may be non-uniform in the axial direction due to the non-uniform magnetic configuration in the tandem mirror. However, as the plug/thermal barrier potential is not actively created in the end-plate biasing experiments, the non-uniformity is expected to be small at least in the long central cell where the fluctuations and the electric potential are mostly measured and analyzed.

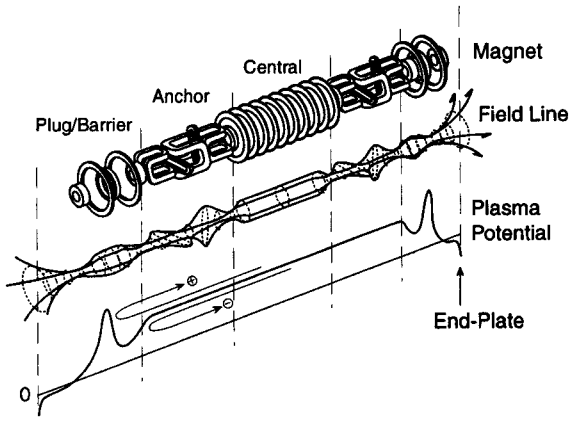

Fig. 1 Schematic of GAMMA10 tandem mirror.

There are two representative modes of operation in GAMMA 10. One is the ECH (Electron Cyclotron Heating) start-up mode and the other is the RF (Radio-Frequency) start-up mode. The ECH mode has a central-cell plasma with lower density of less than 1.0×10^{18} m^{-3} on axis and a higher central-cell potential of around 1 kV with electron temperature higher than 100 eV. The density profile is rather flat near axis and steep near the edge. On the other hand, the RF mode has a peaked central-cell density profile with a relatively higher density of 3.0×10^{18} m^{-3} and a higher ion temperature of around 5 keV.

2.2 Control of E_r in the ECH Mode

In order to control radial electric field of the central-cell plasma, a bias voltage is applied only on #1 and #2 segments of the end plates. Potential profiles are measured by a beam probe [31] in the barrier region for various end-plate biasing. Density fluctuations are measured by a microwave Fraunhofer diffraction method. Density fluctuations, which is concluded to be due to electron drift waves are reduced from 10% to 1% by the increase in radial electric field, irrespective of its sign [11]

2.3 Control of E_r in the RF Mode

A stability boundary for a flute interchange mode based on the average mimimum B criterion has been experimentally confirmed in the RF mode [10], since ion temperature is enough high for diamagnetic loop signals to be measured accurately. Typical ion

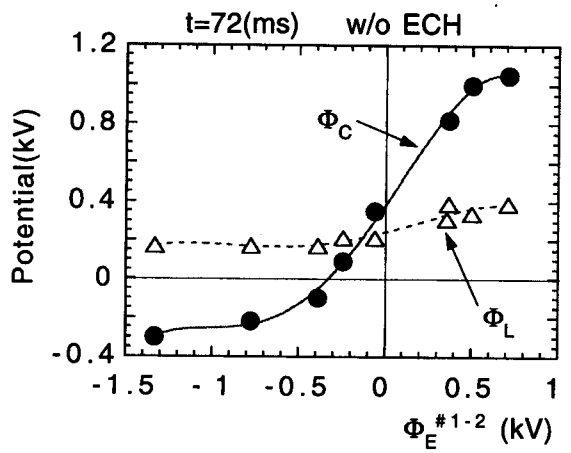

Fig. 2 Central-cell on-axis potential $\Phi_C(0)$ and floated-limiter potential Φ_L versus end-plate potential Φ_E. Radial potential profile is controlled by biasing a voltage on #1 and #2 annular segments of end-plate.

temperature perpendicular and parallel to the magnetic field line is 5 keV and 400 eV, respectively. The stability boundary is determined by a critical beta ratio $\beta_{C\perp}/\beta_{A\perp}$. Here $\beta_{C\perp}$ and $\beta_{A\perp}$ are central-cell beta and anchor-cell beta perpendicular to the field line, respectively. Above the critical ratio, violent density fluctuations appear and the plasma cannot be sustained.

It is found that plasma stability depends not only on the critical beta ratio but also on radial electric field E_r. In Fig.2, on-axis central-cell potential $\Phi_C(0)$ and the limiter potential Φ_L are plotted against the end-plate potential Φ_E biased on #1 and #2 segments. Only the on-axis plasma potential is available, because the gold neutral beam probe in the central cell cannot be radially scanned. Positive and negative radial potential differences $\Delta\Phi_C = \Phi_C(0) - \Phi_{EG}$ in Fig.2 correspond to hill-type and well-type potential profile, respectively. Here, the edge plasma potential Φ_{EG} is estimated from the floating potential of the central-cell limiter Φ_L together with the edge electron temperature T_e of 25 eV by using $\Phi_{EG} = \Phi_L + 3T_e$.

When the plug-ECH power is injected for the plug potential formation, the central-cell diamagnetic signal often decreases and edge-fluctuations on Langmuir-probe current suddenly increase as seen in Fig.3(a). Edge fluctuations are not necessarily correlated to the ECH power injection. As shown in Fig.3(b), the edge activities are suppressed by end-plate biasing even during the ECH power injection. This shows clearly that the radial electric field is responsible for low-frequency

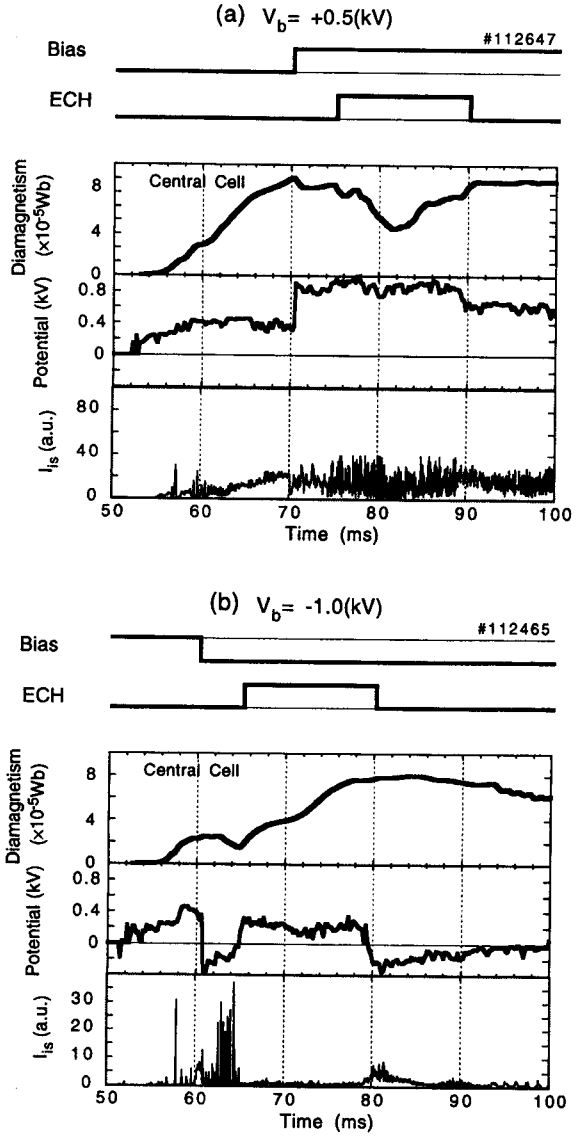

Fig. 3 Effects of end-plate biasing and plug-ECH injection on diamagnetism, on-axis potential $\Phi_C(0)$ and egde fluctuations on probe current I_is in the central cell. (a) biasing voltage V_b = +0.5 kV, (b) V_b = –1.0 kV.

edge fluctuations.

For a given value of the perpendicular beta ratio $\beta_{C\perp}/\beta_{A\perp}$, the central-cell plasma is sustained for the full duration for a certain range of the radial potential difference $\Delta\Phi_C$. These results are plotted by open circles in Fig.4 . It is clearly seen that there is a critical boundary on the perpendicular beta ratio $\beta_{C\perp}/\beta_{A\perp}$ indicated by a broken line, above which the plasma cannot be sustained. The critical beta ratio has its peak near $\Delta\Phi_C = 0$, that is, zero radial electric field and

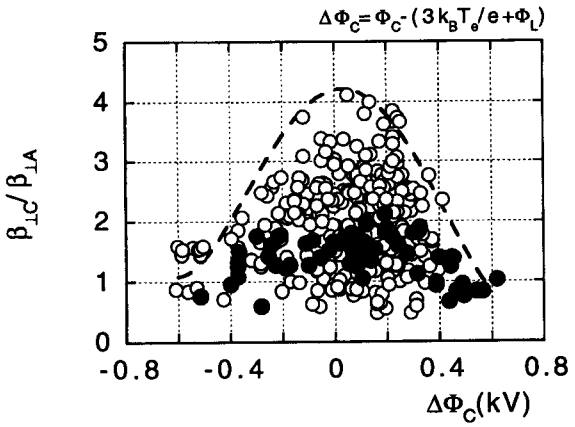

Fig. 4 Perpendicular beta ratio $\beta_{C\perp}/\beta_{A\perp}$ versus radial potential difference $\Delta\Phi_C = \Phi_C(0) - \Phi_{EG}$. Broken line is an experimentally-determined envelope above which the plasma dumps. Solid circles correspond to the data which are FFT-analyzed to identify modes of fluctuations shown in Fig.5.

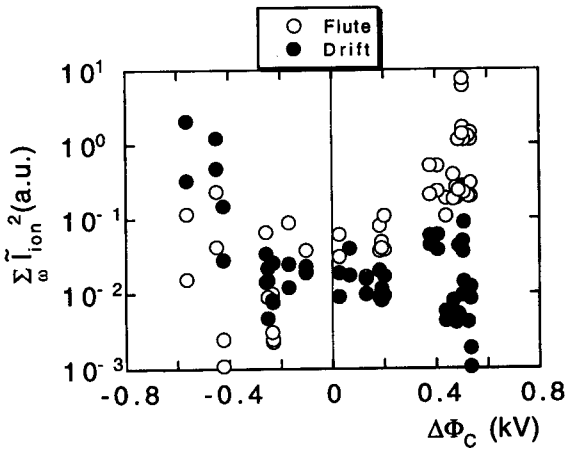

Fig. 5 Dependence of fluctuation level on radial potential difference $\Delta\Phi_C = \Phi_C(0) - \Phi_{EG}$ for shots with beta ratio between 1 and 2 indicated by solid circles in Fig.4.

decreases with an increase in E_r, irrespective of its sign. This means that there is a stability window with respect to $\Delta\Phi_C$.

Fluctuations in the edge plasma are measured by use of an azimuthal array of electrostatic probes set on the central-cell limiter. Fluctuations are FFT-analyzed in order to clarify dependence of the fluctuation level on the radial electric field by selecting shots with the beta ratio between 1 and 2, which are indicated by solid circles in Fig.4. The results are shown in Fig.5. The fluctuation levels is kept low in the weak E_r region and increase drastically when E_r increases, leading to the plasma-dump. Comparing Fig.4 with Fig.5, it is clearly seen that the larger the beta ratio $\beta_{C\perp}/\beta_{A\perp}$ is, the narrower the stability window is.

In order to identify modes of instabilities, phase velocity v_{ph} is experimentally obtained from the phase spectral analyses of the fluctuations. Two modes of instabilities are identified; one is drift mode with azimuthal mode number m = 1, propagating in the electron diamagnetic direction and the other is m = 1 flute mode rotating with $\boldsymbol{E} \times \boldsymbol{B}$ drift velocity. The flute mode and drift modes are discriminated by open and solid circles, respectively, in Fig.5. It is concluded from a limited number of available data the flute modes are dominated in strong positive E_r, while the electron drift modes are in strong negative E_r. It should be noted that the stability window on $\Delta\Phi_C$ seems to be symmetric with respect to $\Delta\Phi_C$ = 0 but different modes of fluctuations are dominated in the region of $\Delta\Phi_C > 0$ and $\Delta\Phi_C < 0$, as seen in Fig.5.

In GAMMA10, effect of $\boldsymbol{E} \times \boldsymbol{B}$ drift shear cannot be discussed due to the lack of the precise radial potential profile up to the plasma edge in the central cell. It should be noted that the potential profile attained in the RF mode of GAMMA10 by keeping all of the end-plate segments floating is actually very effective to keep the radial electric field weak and to suppress low-frequency fluctuations in the central cell, because in this case most of the radial potential drop appears on the end-plate segments instead of appearing in the central cell.

3. Control of E_r and Its Shear in the Q_T-U Device

3.1 Q_T-U Linear Device

The experiment is performed in the Q_T-U linear device of Tohoku University [14], whic is shown in Fig.6. An argon plasma with electron density $n_e = 10^{16}$ m^{-3}, electron temperature T_e = 7 eV and ion temperature T_i = 1 eV is produced by electron cyclotron resonance (ECR) heating. Magnetic field strength is almost uniform and 2.3 kG in the experimental region except for in the ECR plasma source region. Profiles of electron density, electron temperature and space potential are measured by Langmuir probes. Radial profile of density in the experimental region is rather flat near axis and has a steep gradient near the edge. Flute and drift mode instabilities are identified by FFT-analyzing the observed fluctuations for various E_r and its shear. Flute-mode and drift-mode fluctuations are

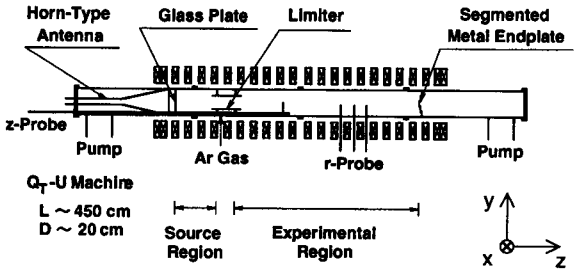

Fig. 6 Schematic of Q_T-U device.

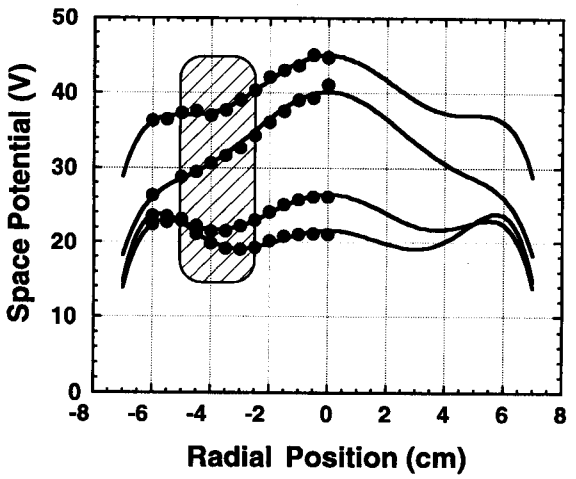

Fig. 7 Typical profiles of radial potential in Q_T-U. Both electric field and its shear are varied. Fitted curves are 6th-order polynomials.

localized mainly in the radial region with steep density gradient.

The end-plate has ten concentric rings in order to precisely control both radial electric field and its shear in a wide range [15]. The radial electric field is confirmed to be axially uniform in the experimental region. Radial electric field E_r and its shear are obtained by fitting 6th-order polynomial functions to the measured plasma potential profiles, as shown in Fig.7. Low-frequency fluctuations are mostly localized in the shadowed region in this figure.

3.2 Effect of E_r and Its Shear on Flute Mode

Rotation frequencies of one mode are almost constant at any radial position, propagating azimuthally in the $\boldsymbol{E} \times \boldsymbol{B}$ direction with azimuthal mode number m = 2. The frequency agrees well with the $\boldsymbol{E} \times \boldsymbol{B}$ drift frequency calculated by using globally-determined electric field. In the axial direction, no phase difference

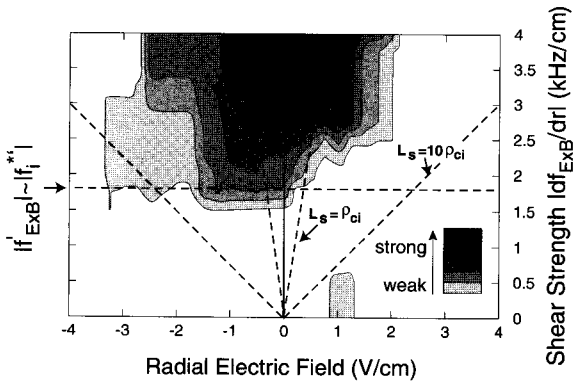

Fig. 8 Contour-plot of flute-mode fluctuation intensities for radial electric field and rotation-frequency shear.

of fluctuations on two probes which are located at axially-different positions is observed within an experimental error. Then it is concluded that these fluctuations are due to flute instabilities which propagate azimuthally with the $\boldsymbol{E} \times \boldsymbol{B}$ rotation frequency. Ion diamagnetic drift frequency is very low in the present plasma due to the low ion temperature. The fluctuation intensities are contour-plotted on the plane of E_r and shear of rotation frequency in Fig.8. The fluctuation intensities increase drastically with the increase in $\boldsymbol{E} \times \boldsymbol{B}$ rotation shear, while those are suppressed by the increase in E_r, regardless of its sign. The slope of a line drawn from the origin is propotional to the inverse of characteristic shear length L. The line on the abscissa means the rigid rotation without any rotation-frequency shear.

The observed instabilitis are driven even at a low rotation frequency as far as the rotation shear is enough strong. The observed frequencies are near the rotaion frequecies which are much lower than those predicted by the IDDEI [27] and the transverse current-driven instabilities [32]. The azimuthal mode numbers larger than m = 2 may be suppressed by the finite Larmor radius effect and The m = 1 mode by the wall effect of the cylindrical metal limiter, which is located between the plasma source region and the experimental region. As shown in Fig.8, the instability grows in the region where the electric field rotation shear is larger than the diamagnetic drift shear and where the shear length L_s is comparable to and larger than the ion Larmor radius ρ_{ci}. From these experimental results, this mode in the Q_T-U device is concluded to be a low-frequency transverse KH instability [5,20].

3.3 Effect of E_r and Iits Shear on Drift-wave Mmode

Frequencies of the other mode of the fluctuations are found to agree with electron diamagnetic drift frequency ($\omega_e^*/2\pi \simeq$ 5 kHz – 13 kHz) which is calculated by using the density profile. From various experiments, these fluctuations are concluded to be due to electron drift-wave instabilities with m = 2. Fluctuation intensities due to the drift-mode depend on both radial electric field and its shear, as shown in Fig.9. The drift-mode is destabilized in the weakly negative E_r region, where the $\boldsymbol{E} \times \boldsymbol{B}$ rotation frequency is around a quarter of the electron diamagnetic drift frequency. In the strong E_r region, the mode is suppressed, regardless of its sign.

When the $\boldsymbol{E} \times \boldsymbol{B}$ rotation shear increases with E_r being fixed, the drift-mode is destabilized once in a weak shear region, attains the maximum amplitudes and then stabilized in the stronger shear region. The $\boldsymbol{E} \times \boldsymbol{B}$ rotation shear at the maximum amplitudes is nearly equal to the estimated ion diamagnetic drift shear in magnitude with opposite sign and therefore the drift shear is effectively cancelled by each other. This suggests the net drift shear defined by the sum of $\boldsymbol{E} \times \boldsymbol{B}$ drift shear and ion diamagnetic drift shear is responsible for suppressing the drift mode.

In the paper [29], the drift wave growth is generally lowered by transverse velocity shear due to the dissipative effects of the IEDD mechanism, while this mode is destabilized by the reactive effects of the IEDD mechanism at a sufficiently large flow shear and the rotation frequency approaching to ion cyclotron frequency. The destabilization and stabilization behavior observed in the Q_T-U seems apparently to be different from this theoretical prediction, although more careful consideration of this mechanism is necessary by taking account of the differences of the geometry as well as the density and electric field profiles.

4. Comparison between GAMMA10 and Q_T-U Results

In the ECH mode of GAMMA10, the drift mode is destabilized in the weak E_r region, as shown in Fig.2, with the maximum fluctuation level near E_r = 0 and stabilized in the stronger E_r region, regardless of its sign [11]. This behavior agrees qualitatively with that of the drift mode observed in the Q_T-U [15], though the maximum fluctuations in Q_T-U are located at a weakly negative E_r. In the strong E_r region, the mode is suppressed, regardless of its sign. These behaviors of

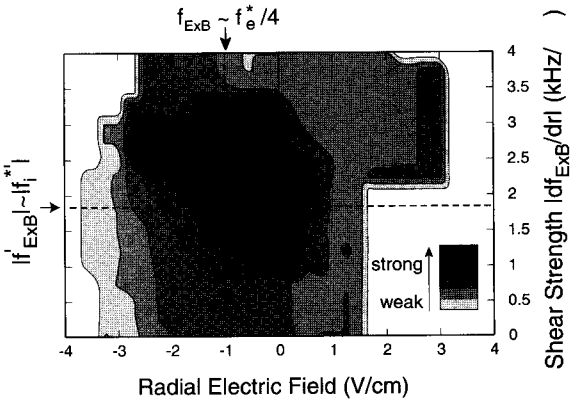

Fig. 9 Contour-plot of drift-mode fluctuation intensities for radial electric field and rotation-frequency shear.

drift modes are consistent with the prediction by Chaudhry et al. [23], though the theory treats a slab model with $\boldsymbol{E} \times \boldsymbol{B}$ shear as well as E_r.

In the RF mode of GAMMA 10, flute modes are strongly excited in the strong positive E_r region, while drift waves are strongly excited in the strong negative E_r region. The experimentally-observed stability window for the flute mode and drift mode seems to be located at $\Delta\Phi_C < 0$ and $\Delta\Phi_C > 0$, respectively, as is expected from Fig.5. These behaviors are consistent with a rotation-driven flute [16] and drift [24] modes, respectively. These E_r dependences in the RF mode are quite opposite to those in the ECH mode of GAMMA 10 and in Q_T-U, where no modes are excited in the strong E_r region, regardless of its sign. On the other hand, in the strong $\boldsymbol{E} \times \boldsymbol{B}$ drift shear region in Q_T-U, Kelvin-Helmholtz mode is excited. These different behaviors in GAMMA10 and Q_T-U may be due to the fact that the magnetic field line in Q_T-U is straight and has almost no curvature, while that in GAMMA 10 has a bad curvature in the central cell. The effect of $\boldsymbol{E} \times \boldsymbol{B}$ drift shear cannot be discussed in GAMMA 10 due to the lack of the precise radial potential profile up to the plasma edge in the central cell.

5. Conclusions

In the ECH mode of GAMMA 10, the drift-mode fluctuation amplitude has its peak near the weak E_r region and suppressed in the strong E_r region, regardless its sign. In the RF mode of GAMMA 10, on the contrary, the flute and drift modes are destabilized in the strong positive and negative E_r region, respectively. These are qualitatively consistent with theoretically-

predicted rotation-driven flute and drift modes.

The flute-mode observed in Q_T-U is identified as a low frequency Kelvin-Helmholtz instability driven by strong $\boldsymbol{E} \times \boldsymbol{B}$ flow shear. Fluctuation intensities due to a drift mode depend on both radial electric field and its shear. The drift-mode is destabilized in the region of weakly negative E_r. In the strong E_r region, the mode is suppressed irrespective of its sign. The drift-mode is clearly stabilized by the increase in the net ion drift shear which is defined as the sum of $\boldsymbol{E} \times \boldsymbol{B}$ drift drift shear and ion diamagnetic drift shear.

Acknowledgements

The author deeply acknowledges the GAMMA10 group of University of Tsukuba and Drs. M. Yoshinuma, T. Kaneko, A. Ando, K. Hattori and Profs. R. Hatakeyama and N. Sato for their collaboration. This work was supported partly by a Grant-in-Aid for Scientific Research from the Ministry of Education, Science and Culture of Japan and partly by the LHD Joint Planning Research Program at National Institute for Fusion Science.

References

[1] F. Wagner *et al.*, Phys. Rev: Lett. **49**, 1408 (1982).
[2] V. Erckmann *et al.*, Phys. Rev. Lett. **70**, 2086 (1993).
[3] O. Sakai *et al.*, Phys. Rev. Lett. **70**, 4071 (1993).
[4] A. Tsushima *et al.*, Phys. Rev. Lett. **56**, 1815 (1986).
[5] D.L. Jassby, Phys. Fluids **15**, 1590 (1972).
[6] K. Odajima, J. Phys. Soc. Jpn. **44**, 1685 (1978).
[7] A. Komori *et al.*, Phys. Fluids. **31**, 210 (1988).
[8] R.J. Taylor *et al.*, Phys. Rev. Lett. **63**, 2365 (1989).
[9] R.R. Weynants *et al.*, Plasma Phys. Control. Fusion **40**, 635 (1998).
[10] M. Inutake *et al.*, *Open Plasma Confinment System for Fusion*, Novosibirsk, 1993, World Scientific, Singapore, 51 (1994).
[11] A. Mase *et al.*, Phys. Rev. Lett. **64**, 2281 (1990).
[12] T. Tokuzawa *et al.*, Jpn. J. Appl. Phys. **33**, 807 (1994).
[13] Y. Kiwamoto *et al.*, Phys. of Plasmas **3**, 578 (1996).
[14] M. Yoshinuma *et al.*, Phys. Letters A **255**, 301 (1999).
[15] M. Yoshinuma *et al.*, *11th Int. Toki Conference*, Toki-city, PI-69, 2000.
[16] M.N. Rosenbluth *et al.*, Phys. Fluids **8**, 1300 (1965).
[17] F.W. Perkins *et al.*, Phys. Fluids **27**, 2067 (1984).
[18] G. Ganguli *et al.*, Phys. Fluids **31**, 823 (1988).
[19] H. Hojo *et al.*, J. Phys. Soc. Jpn **64**, 4073 (1995).
[20] G.I. Kent *et al.*, Phys. Fluids **12**, 2140 (1969).
[21] H. Sanuki *et al.*, Phys. Fluids **27**, 2500 (1984).
[22] H. Hojo *et al.*, J. Phys. Soc. Jpn. **57**, 711 (1988).
[23] M.B. Chaudhry *et al.*, J. Phys. Soc. Jpn. **57**, 3043 (1988).
[24] W. Horton *et al.*, Phys. Fluids **27**, 2067 (1984).
[25] M.E. Koepke *et al.*, Phys. Rev. Lett. **72**, 3355 (1994).
[26] W.E. Amatucci *et al.*, Phys. Rev. Lett. **77**, 1978 (1996).
[27] G. Ganguli, Phys. Plasmas **4**, 1544 (1997).
[28] J.R. Peñano *et al.*, Phys. Plasmas **5**, 4377 (1998).
[29] V. Gavrishchaka *et al.*, Phys. Plasmas **3**, 3091 (1996).
[30] M. Inutake *et al.*, Phys. Rev. Lett. **55**, 939 (1985).
[31] K. Ishii *et al.*, Rev. Sci. Instrum. **60**, 3270 (1989).
[32] M. Yamada *et al.*, Phys. Rev. Lett. **38**, 1529 (1977).